Why Galaxies Care About Spectroscopy

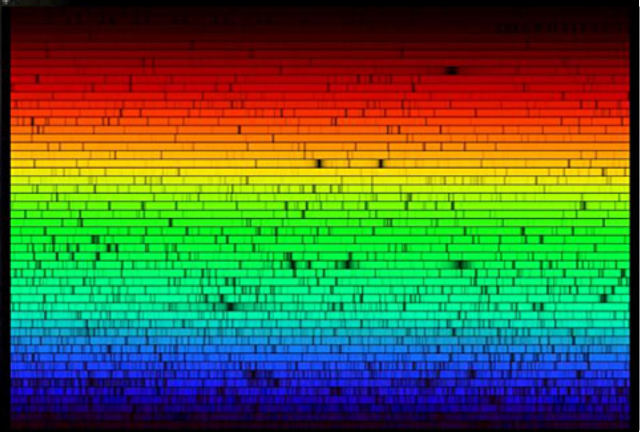

Paul Eigenthaler

Classification

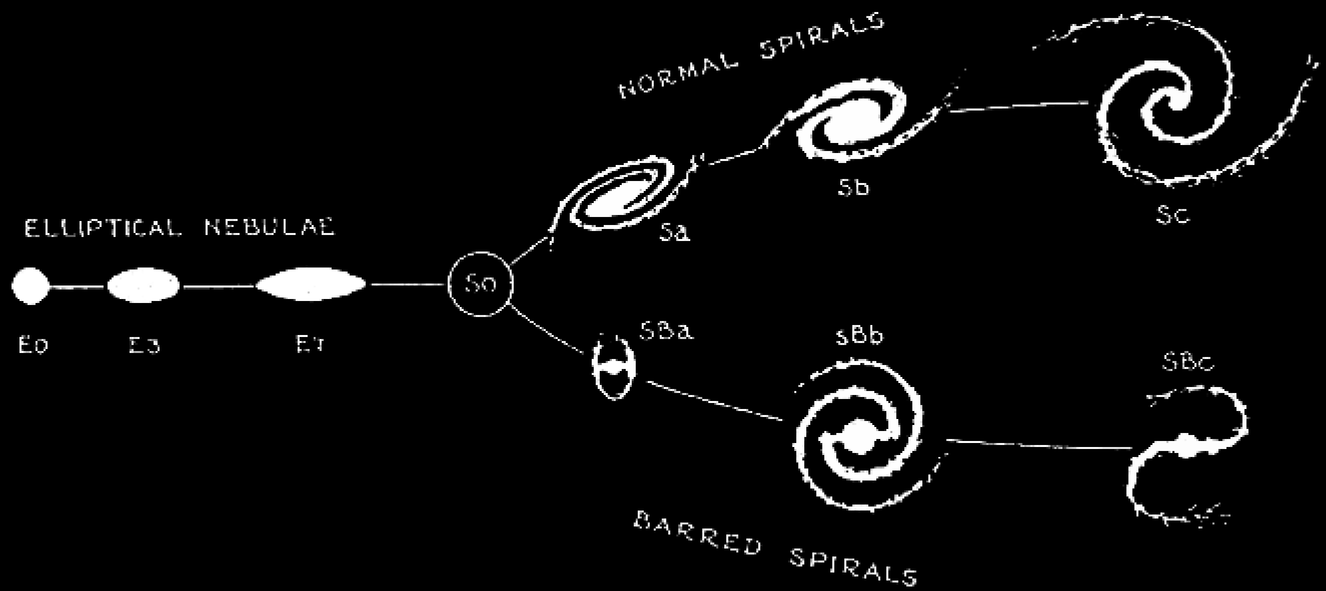

Hubble 1935, *The Realm of the Nebulae*

Classification

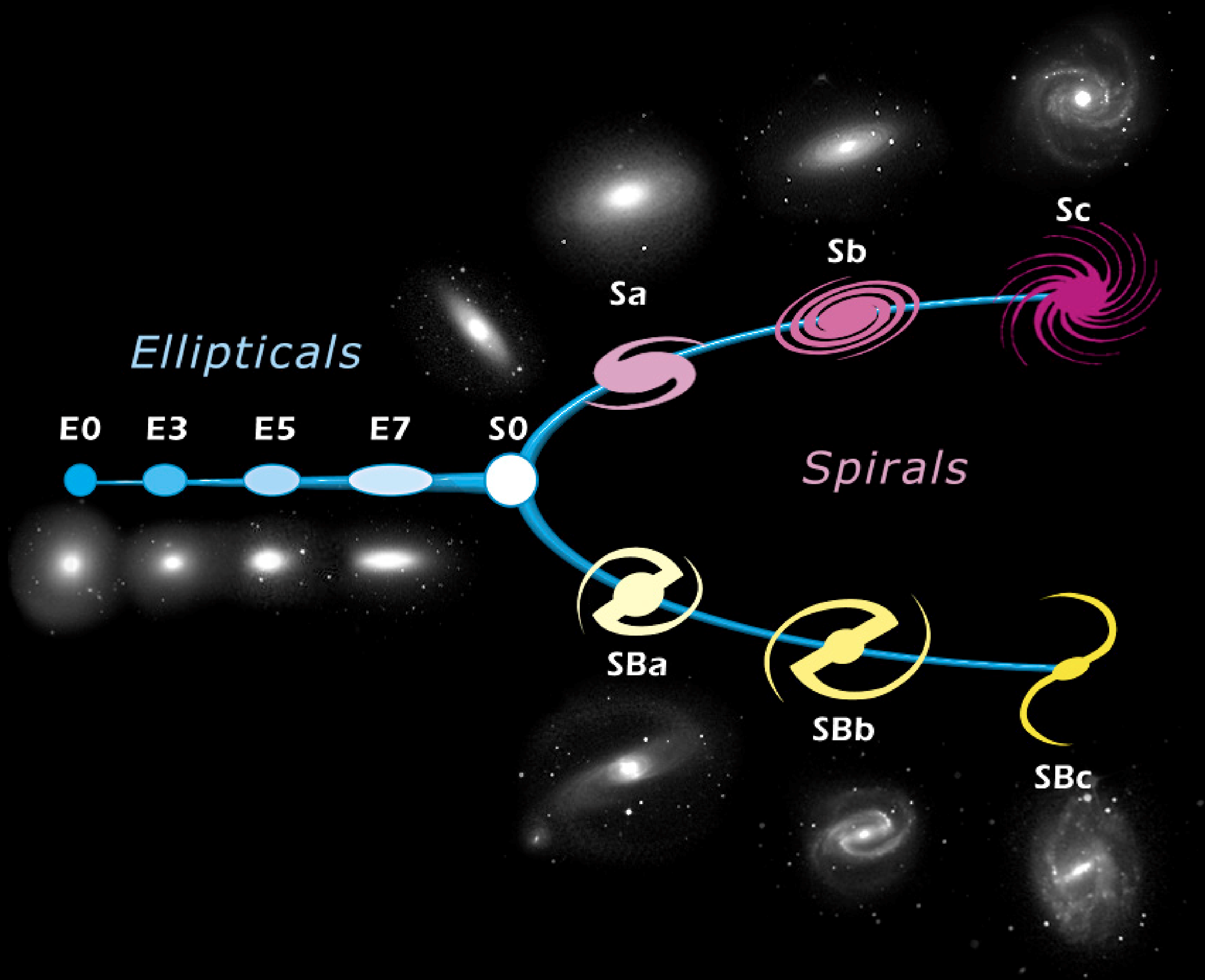

Instrumentation

- Example: VLT FORS1 and FORS2
- visual and near UV FOcal Reducer and low dispersion Spectrograph

Instrument Mode	Mag-limit
Direct Imaging	U=25.2 B=27.1 V=27.0 R=26.6 I=25.5 z=24.3
Imaging Polarimetry	R=23.0

Instrument Mode	Rs = λ/Δλ	Mag-limit
MOS - movable slits [1]	260-1700	R=24.0-22.8
Longslit Spectroscopy [2]	260-1700	R=24.0-22.8
Spectropolarimetry [3]	260-1700	R=19.2-17.2

FORS1

Instrument Mode	Mag-limit
Direct Imaging	U=24.5 B=27.1 V=27.0 R=26.7 I=25.7 z=24.7
HIT imaging	--

Instrument Mode	Rs = λ/Δλ	Mag-limit
MOS - movable slits [1]	260-2600	R=24.2-23.3
MXU - exchangeable masks [2]	260-2600	R=24.2-23.3
Longslit Spectroscopy [3]	260-2600	R=24.2-23.3
HIT spectroscopy [4]	660-780	--

FORS2

Basics

- Radial velocities are measured via the classical Doppler Effect

$v_r = c \cdot z$ $z = \frac{\Delta\lambda}{\lambda_0}$ $\Delta\lambda = \lambda - \lambda_0$ $\lambda = (1+z)\lambda_0$

- relativistic effects important at redshifts $z \geq 0.1$

$\Rightarrow$ relativistic Doppler Effect $v_r = c \cdot \frac{(z+1)^2 - 1}{(z+1)^2 + 1}$

- $\Rightarrow$ Spectroscopy offers the possibility to study the dynamics of galaxies in detail
- drawback: only limited to radial velocity space and no three-dimensional picture

- Hubble Flow $v_r = H_0 \cdot r$ $r = \frac{c \cdot z}{H_0}$ $r\ [\mathrm{Mpc}]$ $[H_0] = \mathrm{km\ s^{-1}\ Mpc^{-1}}$

- At higher redshifts: Luminosity and Angular Diameter Distances

$$D_L(z) = (1+z)^2 \cdot D_A(z)$$

- $\Rightarrow$ redshift allows to determine distances

Seyfert´s Sextet

- Membership confirmation of galaxies in groups and clusters

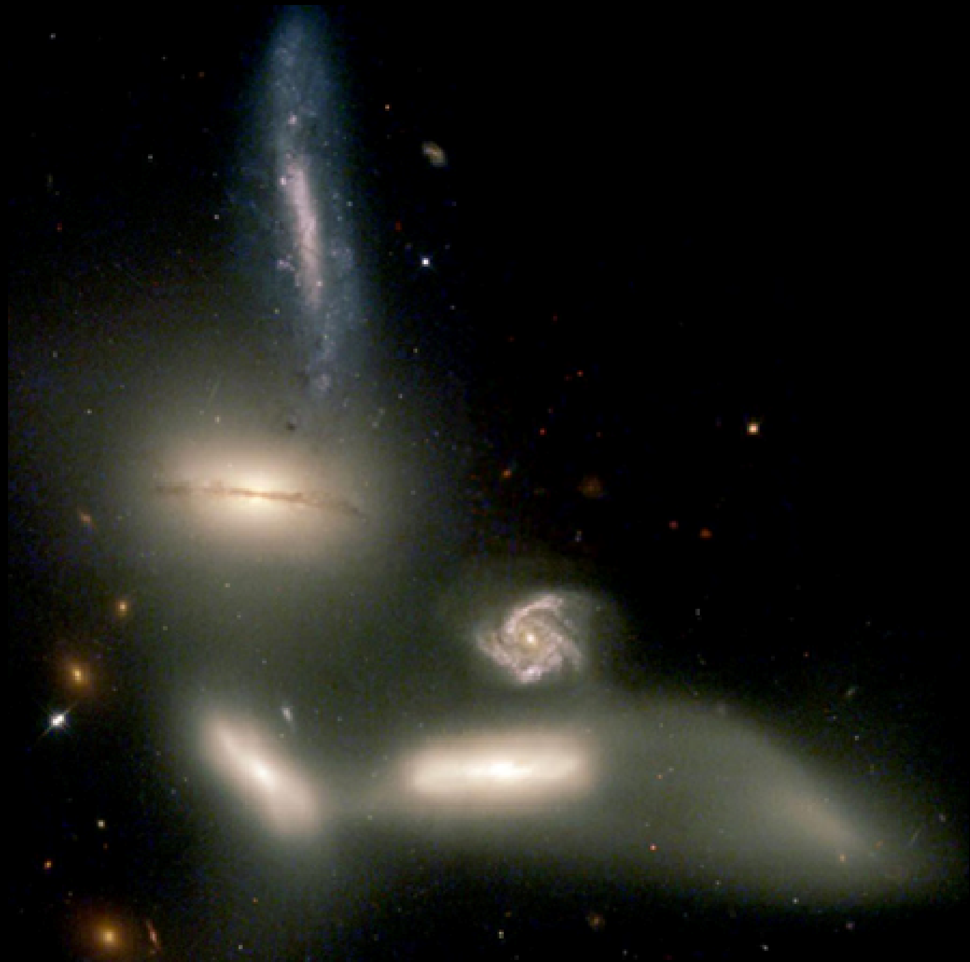

Dynamical Classification

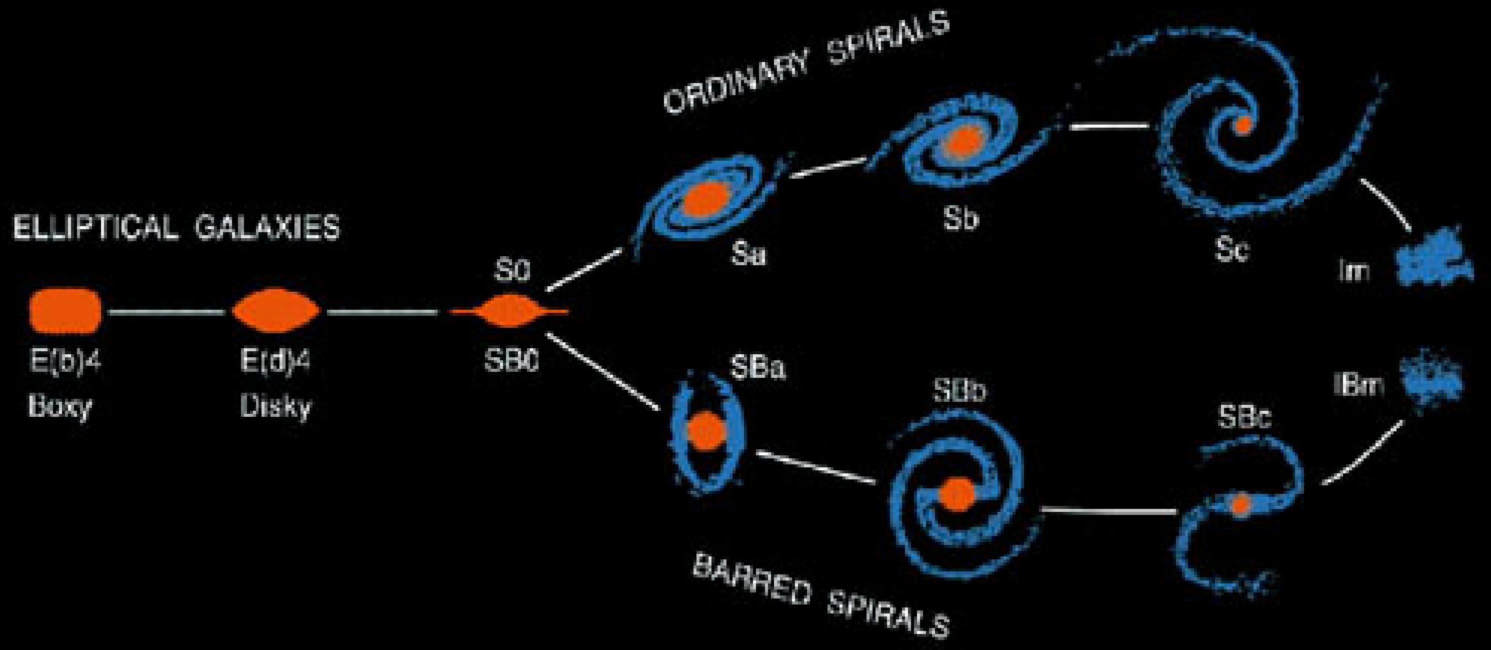

Bender & Kormendy 1996, ApJ 464 119

Dynamics of Spiral Galaxies

NGC 4244

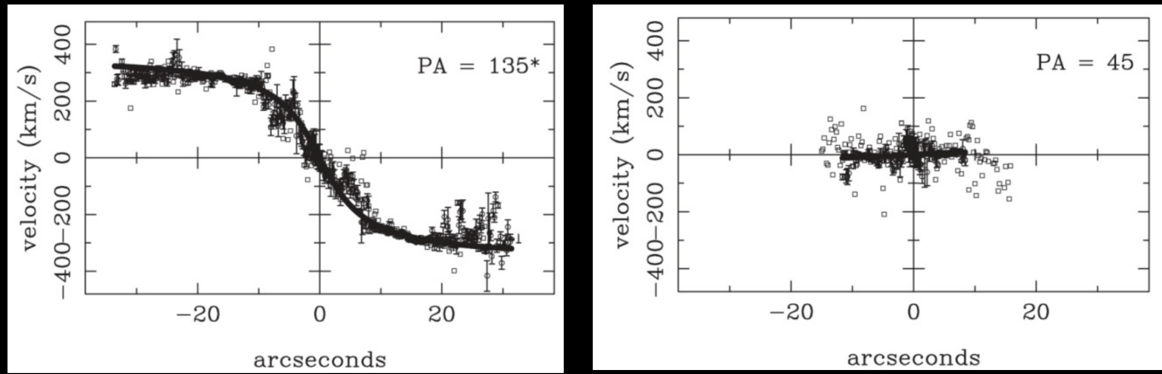

NGC 2639

- long-slit spectroscopy in spiral galaxies reveals rotation curves (dynamically cold)

$\Rightarrow$ determination of virial mass and dark matter content

$$v^2(r) = \frac{G \cdot M(r)}{r}$$

- radial velocity maps „spider-diagrams“

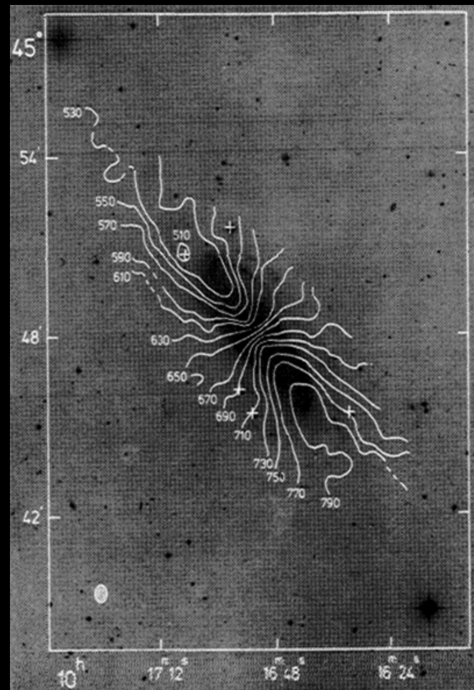

NGC 3198

Rotation Curves

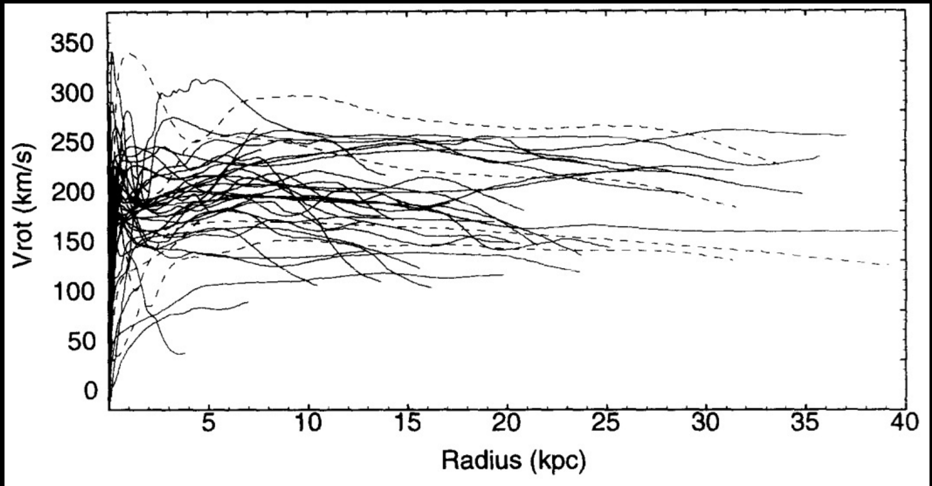

Sofue 1999, AdSpR 23 949

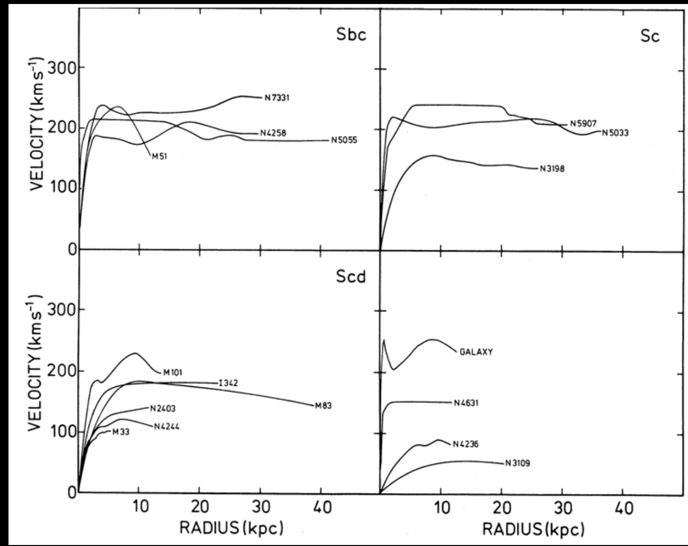

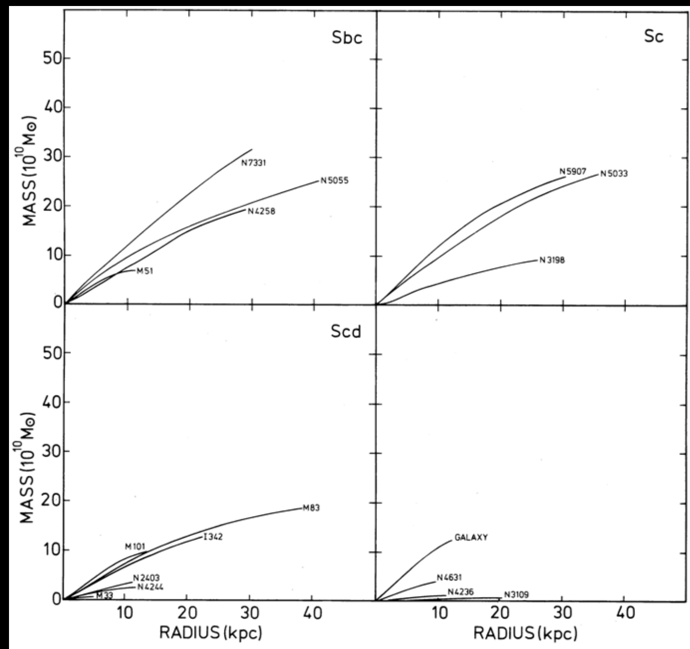

Bosma 1981, AJ 86 1825

- rotation curves increase steeply in the innermost part and flatten outside
- flat rotation curves indicate dark matter

$$v^2(r) = \frac{G \cdot M(r)}{r} \Rightarrow M(r) = \frac{v^2(r) \cdot r}{G}$$

$$\frac{v^2(r)}{G} = \text{const.} \Rightarrow M(r) \propto r$$

Spider Diagrams

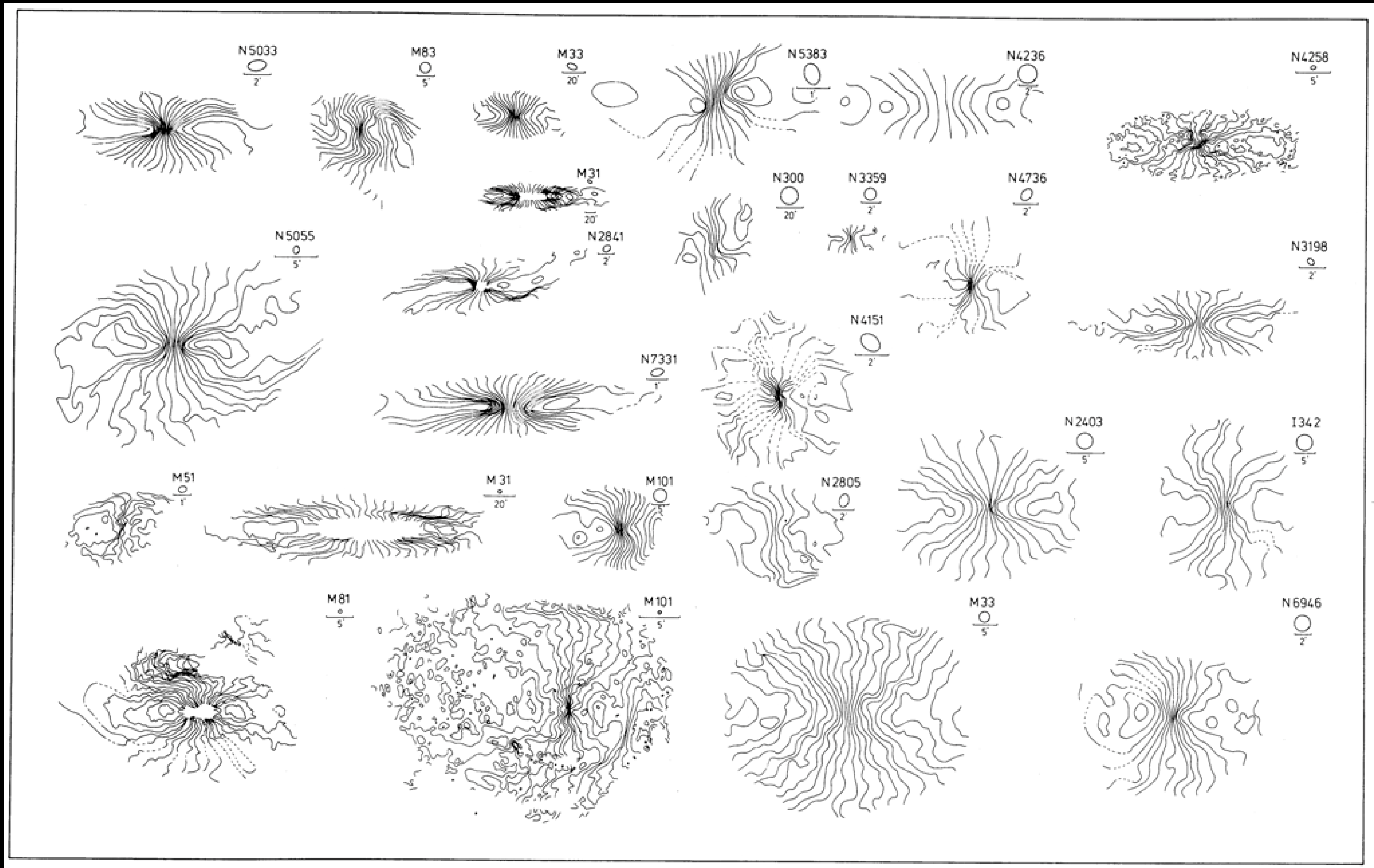

Bosma 1981, AJ 86 1825

Dynamics of Elliptical Galaxies

• in most Es the stellar velocity dispersion σ exceeds the rotation velocity

$\Rightarrow$ elliptical galaxies are pressure-supported rather than rotation-supported systems (dynamically hot)

• high stellar velocity dispersions lead to broadening of absorption features representative for the old stellar population [Ca K, Ca H, Mg, Na, CaII Triplet]

• measure of line broadening via the FWHMs of fitted gaussians or cross correlation with a stellar template (K giants)

$$\chi^2 = \sum [G - B \cdot S]^2$$

M87

• assumption that elliptical galaxies are in virial equilibrium

$\Rightarrow$ virial theorem and velocity dispersion allow to calculate the dynamical mass of the system

$$\sigma^2 = \langle v^2 \rangle \simeq \frac{G \cdot M}{R}$$

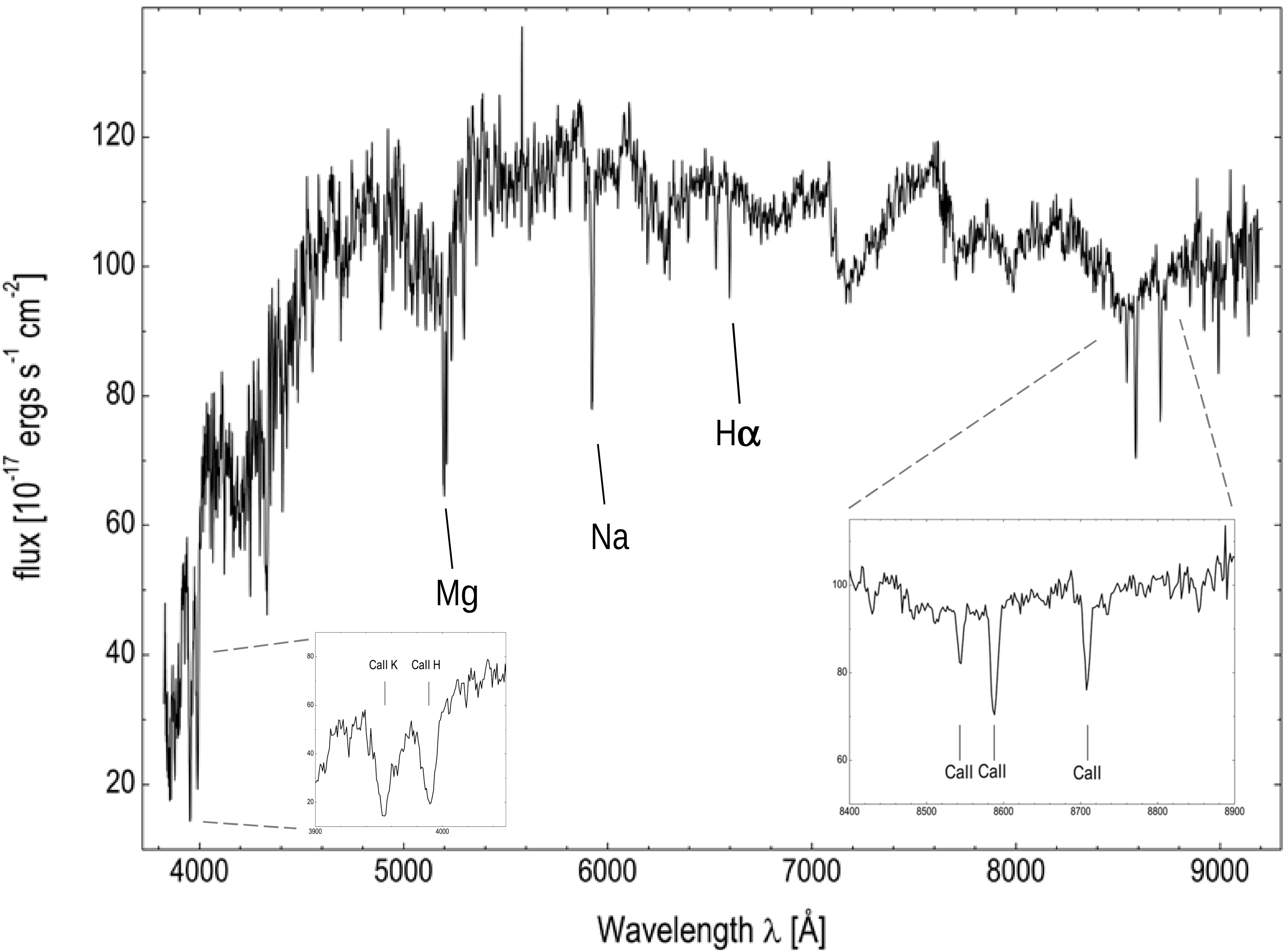

flux [10^-17 ergs s^-1 cm^-2]
Wavelength λ [Å]
Mg
Na
Hα
Call K
Call H
Call Call
Call

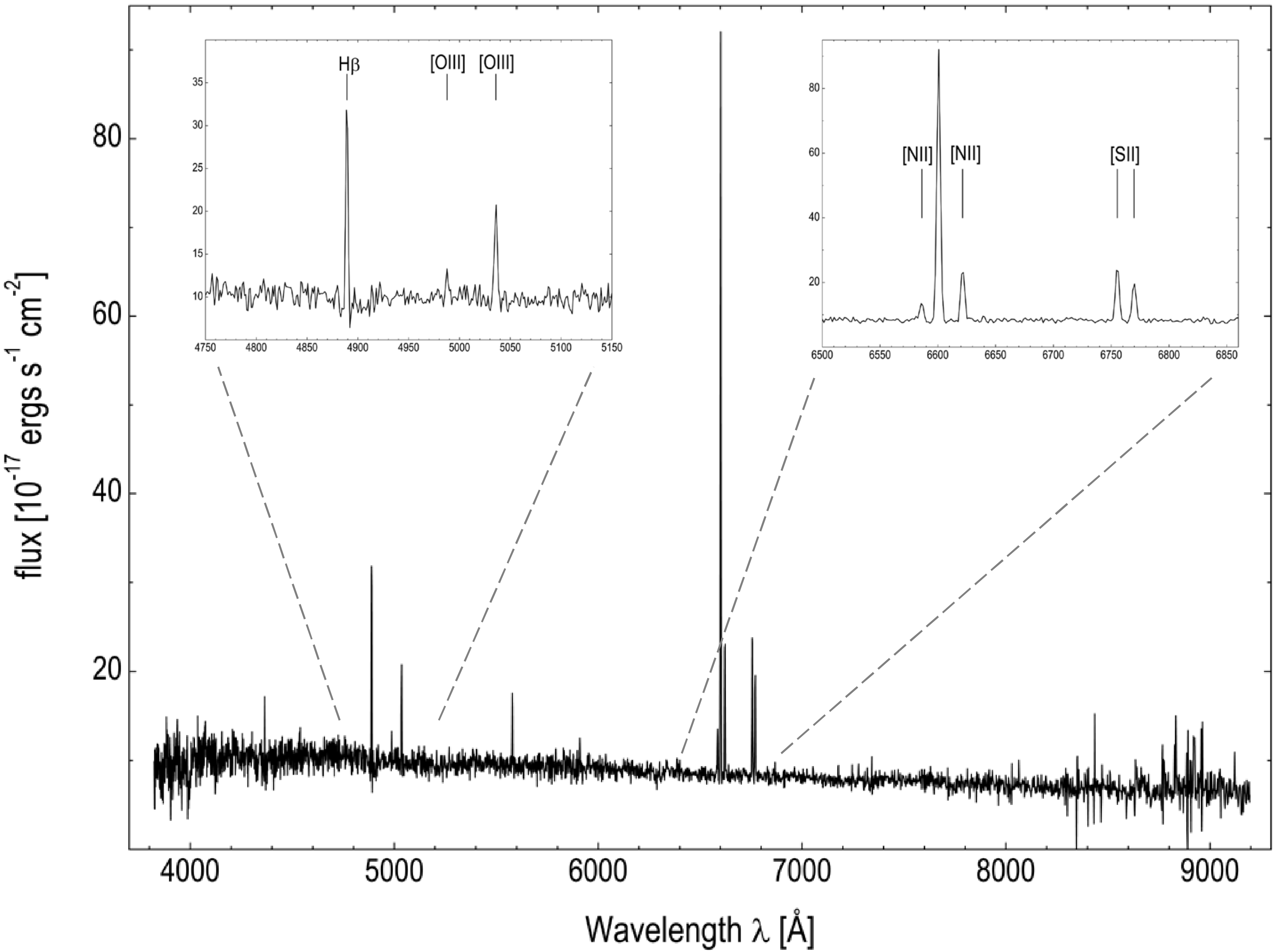

flux [10^-17 ergs s^-1 cm^-2]
Wavelength λ [Å]
Hβ
[OIII]
[OIII]
[NII]
[NII]
[SII]

Analysis of Emission-Line Spectra

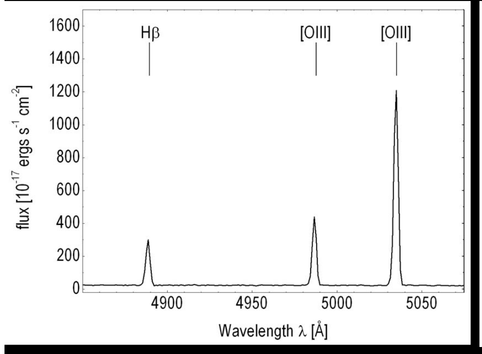

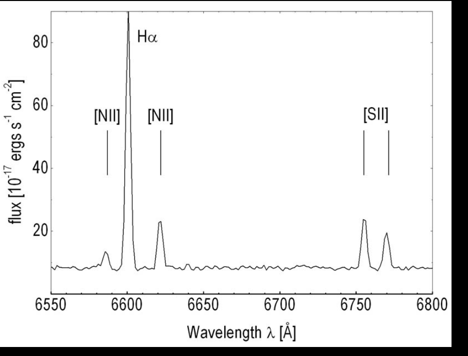

- Hα, Hβ, [OIII], [NII] and [SII] most prominent features in emission-line galaxies
- line flux ratios [NII]/Hα, [OIII]/Hβ and ([SII]+[SII])/Hα are used to determine ionization mechanisms
- Hα fluxes act as instantanious measure of star formation

$$\mathrm{SFR}(M_\odot\ \mathrm{year}^{-1}) = 7.9 \cdot 10^{-42} L(\mathrm{H}\alpha)(\mathrm{ergs\ s}^{-1})$$

- Hα extinction corrections difficult to estimate
- absorption and reddening caused by dust have to be taken into account

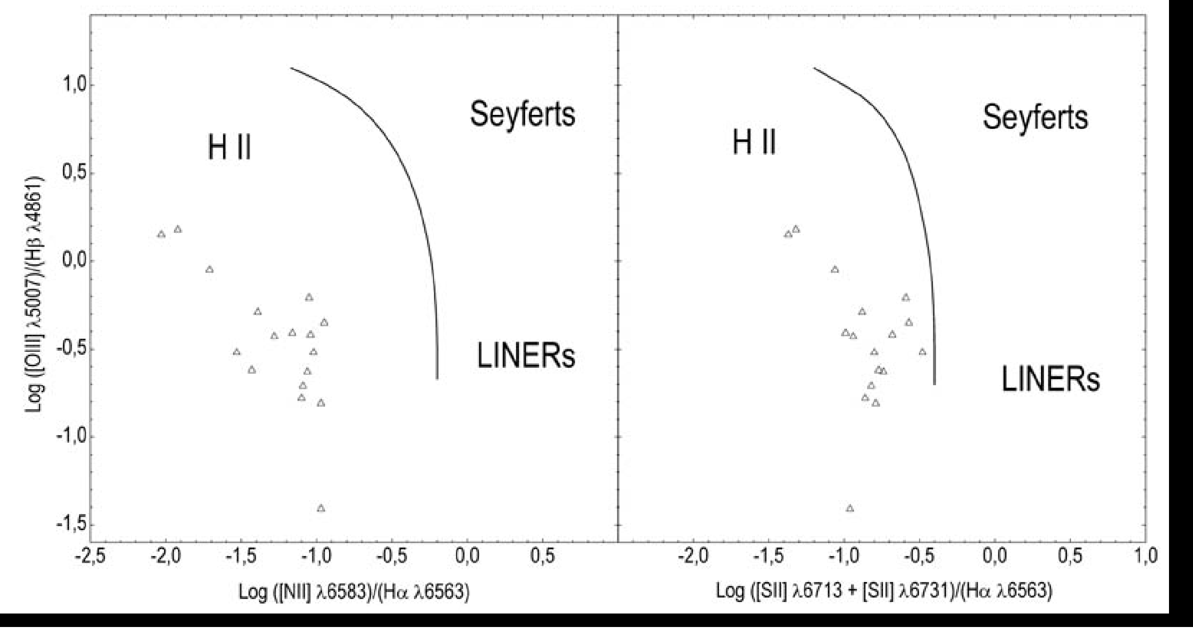

Element Abundances

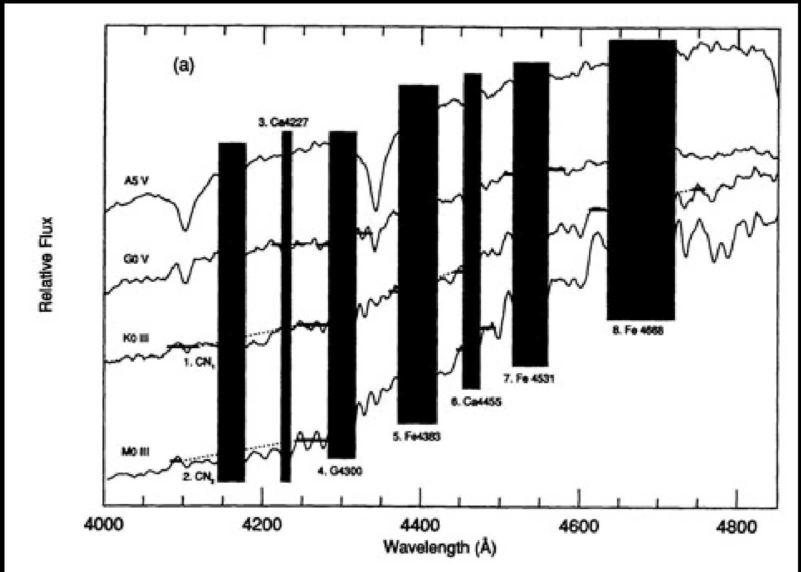

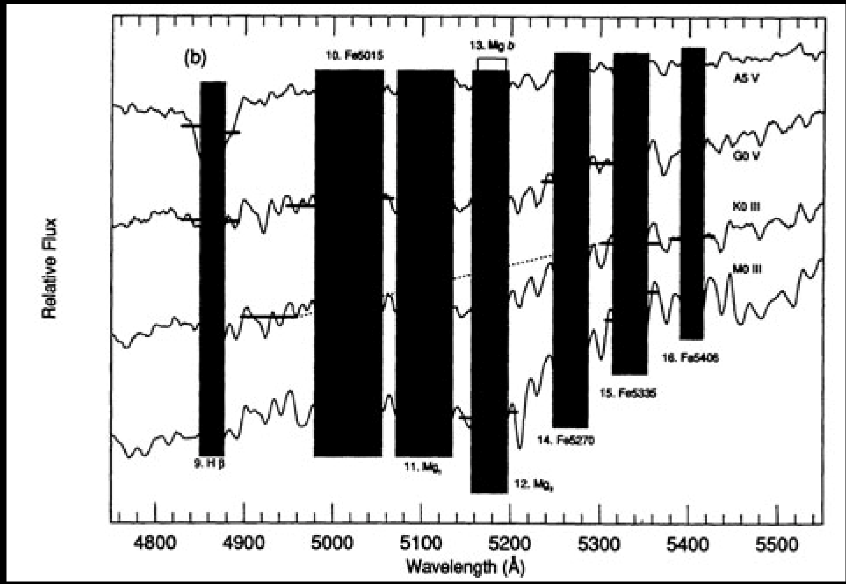

- standards need to be defined to determine element abundances
- Lick IDS System

$$\mathrm{Mag} = -2.5 \log \left[\left(\frac{1}{\lambda_2 - \lambda_1} \right) \int_{\lambda_1}^{\lambda_2} \frac{F_{I\lambda}}{F_{C\lambda}} \, d\lambda \right]$$

- velocity dispersion has to be taken into account when measuring line strengths

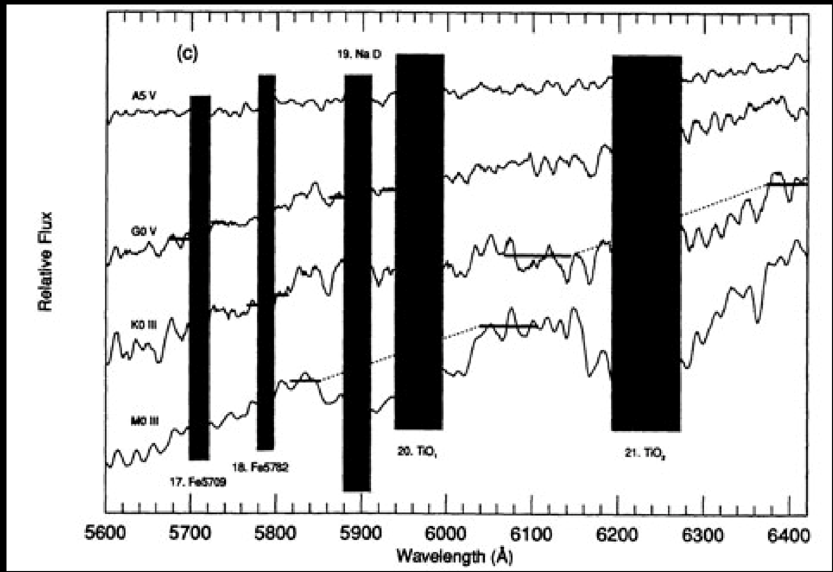

Oxygen Abundances

- Oxygen is the most abundant element after Hydrogen and Helium in the Universe

- different ionization stages (O^+, O^{++}) have to be taken into account when measuring oxygen abundances

$$12 + \log \frac{O^+}{H^+} = \log \frac{I(3726) + I(3729)}{I(H\beta)} + 5.89 + \frac{1.676}{t_e([O\ II])} - 0.40 \log t_e([O\ II]) + \log(1 + 1.35x)$$

$$12 + \log \frac{O^{++}}{H^+} = \log \frac{I(4959) + I(5007)}{I(H\beta)} + 6.174 + \frac{1.251}{t_e([O\ III])} - 0.55 \log t_e([O\ III])$$

$$\frac{O}{H} = \frac{O^+ + O^{++}}{H^+}$$

- if not all oxygen lines can be measured properly, calibrations focusing only on strong lines can be taken into account

- R_{23} Method

$$R_{23} = \frac{I([O\ \text{II}]\ \lambda 3727) + I([O\ \text{III}]\ \lambda\lambda 4959, 5007)}{I(H\beta)}$$

Pagel et al. 1979

- O_3N_2 Method

$$O_3N_2 = \log \left[\frac{I([O\ \text{III}]\ \lambda 5007)/I(H\beta)}{I([N\ \text{II}]\ \lambda 6583)/I(H\alpha)} \right]$$

Alloin et al. 1979

- N_2 Method

$$N_2 = \log \left[\frac{I([N\ \text{II}]\ \lambda 6583)}{I(H\alpha)} \right]$$

Denicoló et al. (2002)

Multi Object Spectroscopy

- Multi Object Spectroscopy (MOS) allows to measure spectra of several sources similarly
- Holes are drilled in an aluminium plate for every single object
- used in All-Sky-Surveys
- most important: Sloan Digital Sky Survey (SDSS)
- SDSS: 5740□^{2}, 674.749 Galaxies
- redshift accuracy: ~30 km s^{-1}

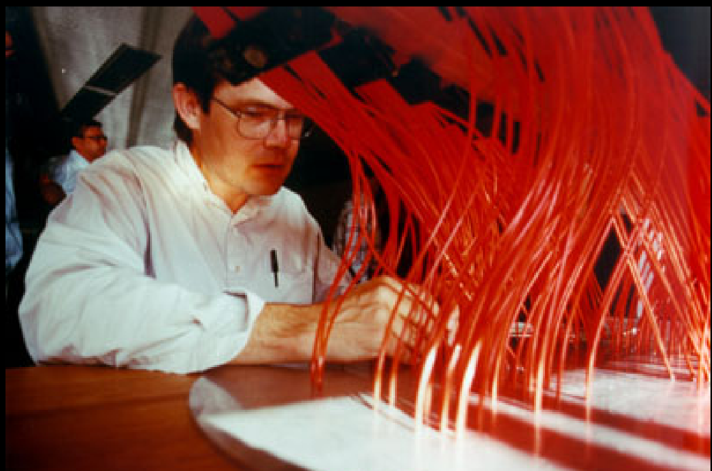

Having fun with fibers ...

Virgo Cluster